Hyperfine Interact (2017) 238:80
https://doi.org/10.1007/s10751-017-1444-4

$DeNO_x$ active iron sites in iron loaded ZSM-5 – a multitechnique analysis of a complex heterogeneous catalyst based on Mössbauer spectroscopy

K. G. Padmalekha[1] · H. Huang[1] · I. Ellmers[2] · R. Pérez Vélez[3] · J. van Leusen[4] · A. Brückner[3] · W. Grünert[2] · V. Schünemann[1]

Abstract Iron loaded zeolites like Fe-ZSM-5 are potent candidates for the catalytic abatement of nitrogen oxides from car exhaust, e.g. from Diesel engines. Recent problems in this field show that there is an urgent need in further improvement of such catalysts, for which a full analysis of Fe species present in them under different conditions is highly desirable. We have studied Fe-ZSM-5 catalysts prepared via solid-state ion exchange by using field dependent Mössbauer spectroscopy at low temperature in order to identify the different iron species present in this type of catalyst in the fresh state and after use in catalysis. Mössbauer spectroscopy proved to be the key technique for a full understanding of species structures, but due to the complexity of structures, guidance by parallel EPR experiments and control by SQUID magnetometry were essential to prove reliability of derived species distributions.

Keywords Fe-ZSM-5 catalyst · Mössbauer spectroscopy · Standard selective catalytic reduction (SCR) · EPR spectroscopy

This article is part of the Topical Collection on *Proceedings of the International Conference on the Applications of the Mössbauer Effect (ICAME 2017), Saint-Petersburg, Russia, 3–8 September 2017* Edited by Valentin Semenov

Electronic supplementary material The online version of this article (https://doi.org/10.1007/s10751-017-1444-4) contains supplementary material, which is available to authorized users.

✉ V. Schünemann
schuene@physik.uni-kl.de

[1] Department of Physics, University of Kaiserslautern, 67663 Kaiserslautern, Germany

[2] Lehrstuhl Technische Chemie, Ruhr-Universität Bochum, Universitätsstraße 150, 44801 Bochum, Germany

[3] Leibniz-Institut für Katalyse e. V., 18059 Rostock, Germany

[4] Institut für Anorganische Chemie, RWTH Aachen, 52056 Aachen, Germany

Published online: 23 October 2017

1 Introduction

Fe-ZSM-5 catalysts have been known to be superior in their catalytic abilities in processes like reduction of nitrogen oxides (NO_x) to N_2 by NH_3 in presence of oxygen (selective catalytic reduction, SCR) [1, 2]. Such reduction reactions are the basis of NOx abatement in the purification of exhaust gasses from diesel engines. Reduction of NO or of NO/NO_2 mixtures, differing drastically in rate and probably in the catalyst sites employed [3], both proceed on Fe zeolites and are differentiated as "standard" and "fast" SCR" [4, 5].

Identification of active iron-sites in heterogeneous Fe-ZSM-5 catalysts is a demanding task because after iron loading and pretreatment the catalyst may contain iron as iron oxide particles (ordered or non-ordered), as single ions in different sites or even as clusters of only a few iron centers [6, 7]. Iron oxide nanoparticles can be formed on the external crystal faces or nearby inside causing structural damage. Small clusters may be hosted in the channels of the ZSM-5 structure whereas the locations for high spin ferric iron ions are in dedicated lattice sites called α-, β-, and γ-sites. Charged metal ions in these sites are exchangeable via ion exchange both by solid-state reaction or in liquid slurry solutions [8–10].

In a previous work it has been derived from in-operando EPR and UV-Vis spectroscopy [9] that ferric high spin Fe^{III} located in the β-sites and a part of Fe^{III} located in the γ-sites may be the active species in fast SCR, but are permanently reduced to inactive Fe^{II} during standard SCR. During fast SCR, they are kept in their active Fe^{III} state by reoxidation with NO_2. For standard SCR, isolated sites remaining Fe^{III} in the feed are considered active sites as well, but a more significant contribution is expected from the small (oligomeric) clusters [11, 12]. However, these assignments are strongly debated [2]. Therefore, a comprehensive analysis of Fe sites in zeolites was highly needed.

EPR spectroscopy is a valuable tool to characterize half integer spin Kramers systems like ferric high and low spin Fe^{III} but Fe^{II} ions are EPR silent. Also, the quantification of the amount of the different Fe^{III} species in complex systems like heterogeneous catalysts is tedious especially if superparamagnetic particles are present which strongly influence the EPR baseline making spin quantification almost impossible.

Therefore, we have used Mössbauer spectroscopy on ^{57}Fe labeled ZSM-5 catalysts together with EPR spectroscopy and complimentary magnetometry in order to identify and determine the different amounts of iron species in Fe-ZSM-5 before and after catalytic standard SCR (sSCR) experiments. In order to do so we developed a methodical approach which involves the spin-Hamiltonian formalism [13] including powder averaging for the paramagnetic Fe^{III} and Fe^{III} species and conventional analysis with Lorentzian line shape for the oxidic phases present in the catalyst.

2 Materials and methods

Isotopically enriched iron was introduced into the zeolite via a gas-phase technique (solid-state ion exchange [14]) and has been characterized before and after standard selective catalytic reduction (sSCR) [4, 5] by Mössbauer and EPR spectroscopy. In total 2 samples labeled **A** and $\mathbf{A_{SCR}}$ have been studied, which were prepared according to the following routes:

A: NH_4-ZSM-5 initially exchanged with calcium chloride solution, after drying and calcination at 500 °C dry introduction of ^{57}Fe (see above). Before analysis dehydrated in He at 150 °C for 1 hour. The exchange degree of protons by Ca was 0.524 and the Fe content was 0.96 wt %.

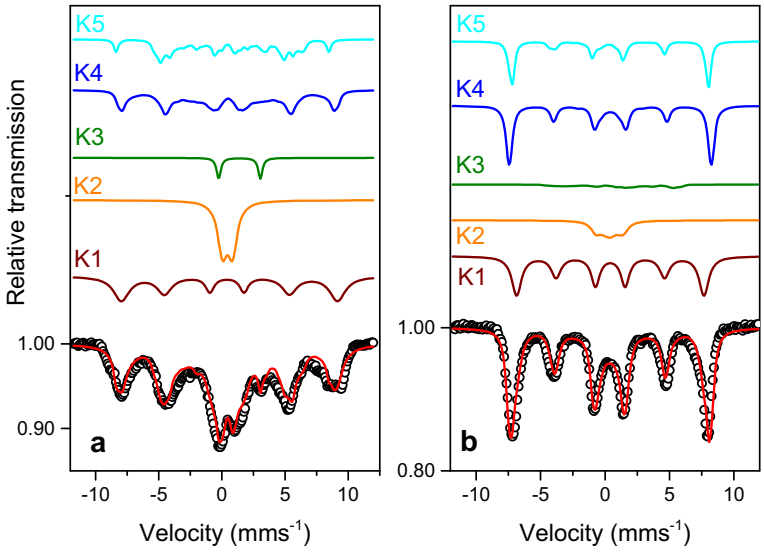

Fig. 1 Mössbauer spectra of sample A before sSCR obtained at T=5 K and B=10 mT (**a**) and B=5 T (**b**). The red solid line is the result of a simulation procedure using 5 different iron species K1 – K5 as described in the text. The relative contribution of K1 – K5 including the obtained Mössbauer parameter sets are given in Table 1

A_{SCR}: Sample **A** after sSCR for 400 °C for 45 minutes, quenched in flowing He; after storage again dehydrated in Helium at 150 °C.

For reference purposes, an additional sample **B** was made using a liquid-phase technique for introduction of ^{57}Fe (Improved Liquid Ion Exchange [11]). This sample, which contained 0.29 wt.% Fe, was studied only in the dehydrated state.

Mössbauer spectroscopy was performed using a closed cycle Helium cryostat equipped with a superconducting magnet described elsewhere [15]. The measurements were done at T= 5 resp. 6 K and 10 mT and 5 T magnetic fields, the magnetic field being parallel to the γ-ray. The resulting multi-component spectra were simulated using Vinda add-on for Excel 2003 [16]. The spin-Hamiltonian formalism including powder averaging was used to simulate the Mössbauer spectra of paramagnetic and diamagnetic iron species [17].

The magnetic properties of samples **A** and **B** were also investigated with a Quantum Design MPMS-5XL SQUID magnetometer. Magnetization was measured at 2 K in magnetic fields between 0 and 5 T. The SQUID data were corrected for diamagnetic contributions of the sample holders. To account for the magnetism of the Fe impurity in technical zeolites (on the order of 0.025 wt-%), the parent H-ZSM-5 was investigated as well, and its contribution was subtracted from the raw data of the ^{57}Fe-ZSM-5 samples assuming that the structure of impurity Fe was not affected during introduction of the ^{57}Fe species. As the correction accounted for ≈10 % of the total magnetism at maximum, uncertainty introduced by such assumption was considered acceptable.

3 Results and discussion

Figure 1 shows the Mössbauer spectra of the ^{57}Fe-ZSM-5 sample **A** obtained at T=5 K in fields of B=10 mT (Fig. 1a) and B= 5 T (Fig. 1b). The low field spectrum exhibits

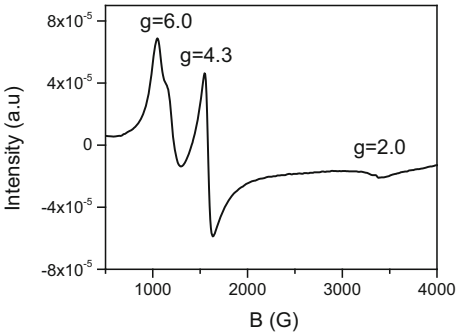

Fig. 2 X-band EPR spectrum of sample A taken at 77 K at a microwave frequency of 9.6 GHz

a complicated magnetic structure with more than one magnetic species present as evident from the inspection of the outer wings of the spectrum. In addition, a central doublet around 0.5 mms^{-1} with a low quadrupole splitting characteristic for ferric high spin iron as well as a line at $\sim$ 3 mms^{-1} indicative for the presence of a ferrous high spin species is observed by inspection of the experimental data.

More information about the magnetic species comes from X-band EPR spectroscopy (s. Fig. 2) which shows the presence of two paramagnetic ferric high-spin iron species. The EPR spectrum shows a signal at a g-factor $\sim$ 6 which can be assigned to paramagnetic ferric high spin ions with S = 5/2 located in an almost axial ligand field exhibiting a rhombicity parameter of E/D $\sim$ 0. Such EPR signals have been assigned to iron ions residing at the β-positions in the ZSM-lattice [9]. In addition, there is a signal at g = 4.3 which stems also from a ferric high spin iron species with S = 5/2 but with a full rhombic ligand field (E/D = 0.33). These ions are located at the γ-position of the ZSM-5. An isotropic EPR signal around g=2 is not evident –the negative bump corresponds to the third g-value of the almost axial signal S=5/2 ions in the β-positions, therefore the corresponding α-sites are populated to an extremely small extent and were neglected in the Mössbauer analysis.

These observations motivated us to analyze the Mössbauer spectra of **A** by using contributions from in total 5 iron species with the parameters listed in Table 1: (i) Large magnetically blocked iron oxide particles (K1) located probably on the surface of the zeolite grains (29% at 10 mT and 38% at 5 T); (ii) diamagnetic μ-oxo bridged Fe^{III} oligomers (K2) (18% at 10 mT and 9% at 5 T); Diamagnetic" meaning that the ground states of the species represented by K2 are characterized by a total spin of S = 0, and excited states are insignificantly populated at 5 K; (iii) paramagnetic Fe^{II} with S = 2 (K3) (3%); (iv) paramagnetic Fe^{III} with S = 5/2 in a fully rhombic ligand field (E/D=0.33) (K4) (30%) as well as (v) a second paramagnetic Fe^{III} with S = 5/2 in an axial ligand field (E/D$\sim$ 0) (K5) (20%). It should be noted that the K2 contribution changes in the field: There are apparently both diamagnetic oligomers (e.g. oxygen-bridged dimers, which had been postulated in literature quite early [18]), but also oligomers containing a higher number of Fe ions, which respond to the field. It is for the first time, that these species have been clearly identified and can now be even quantified.

Magnetometric data of **A** is displayed in Fig. 3. In this diagram, the magnetization is already normalized to the Fe content, i.e. the molar magnetization per mole Fe is plotted, which translates to the magnetic moment per Fe ion by division by the Avogadro number (N_A). With increasing fields, magnetization grew rapidly toward or even beyond 3 $N_A\mu_B$, but was unexpectedly not saturated at 5.0 T, which raised the need for an extrapolation. Based on the plausible assumption that saturation would have been achieved at 10 T, the

Table 1 Mössbauer parameters of the simulations shown in Figs. 1 and 4

Sample	T (K), B (T)	Comp.	δ (mms^{-1})	ΔE_Q (mms^{-1})	Γ (mms^{-1})	B_{hf} (T)	S	D (cm^{-1})	$\frac{E}{D}$	$\frac{A}{g\mu_n}$ (T)	Rel. area (%)
A	**5 K, 10 mT**	K1	0.5	0.2	1.2; 1.1; 0.8	53					29
		K2	0.45	0.79	0.9						18
		K3	1.4	3.3	0.4		2				3
		K4	0.5	0.42	0.5		5/2	0.004	0.33	–21.5; –21.5; –21.5	30
		K5	0.4	-0.7	0.4		5/2	0.5	0.05	–21; –21; –21	20
	5 K, 5 T	K1	0.5	0	0.9; 0.9; 0.8	45					38
		K2	0.45	0.79	0.9						9
		K3	1.4	3.3	0.4		2	–0.11	0	–10.9; –18; –9.5	3
		K4	0.5	0.42	0.5		5/2	0.004	0.33	–21.5; –21.5; –21.5	30
		K5	0.4	-0.7	0.4		5/2	0.5	0.05	–21; –21; –21	20

Table 1 (continued)

Sample	T (K), B (T)	Comp.	δ (mms^{-1})	ΔE_Q (mms^{-1})	Γ (mms^{-1})	B_{hf} (T)	S	D (cm^{-1})	$\frac{E}{D}$	$\frac{A}{g\mu_n}$ (T)	Rel. area (%)
A_{SCR}	**6 K, 10 mT**	K1	0.5	0.2	1.0; 0.8; 0.7	52					42
		K2	0.45	0.79	0.5						8
		K3	1.35	3.3	0.53		2				35
		K4	0.5	0.42	0.5		5/2	0.004	0.33	–21.5; –21.5; –21.5	15
	6 K, 5 T	K1	0.5	0	0.8; 0.67; 0.65	52					43
		K2	0.45	0.79	0.5						7
		K3	1.35	3.3	0.53		2	–0.11	0	–10.9; –18; –9.5	35
		K4	0.5	0.42	0.5		5/2	0.004	0.33	–21.5; –21.5; –21.5	15

The subspectra of K3, K4, and K5 have been simulated by the spin-Hamiltonian approach using the spin S, the zero field splitting parameter D, rhombicity parameter E/D and the hyperfine coupling tensor A given in units of $g_n\mu_n$. Subspectra K1 and K2 have been analyzed using the usual lorentzian line shape model. The color code of the components K1-K5 correspond to the colors of the subspectra shown in Figs. 1 and 4

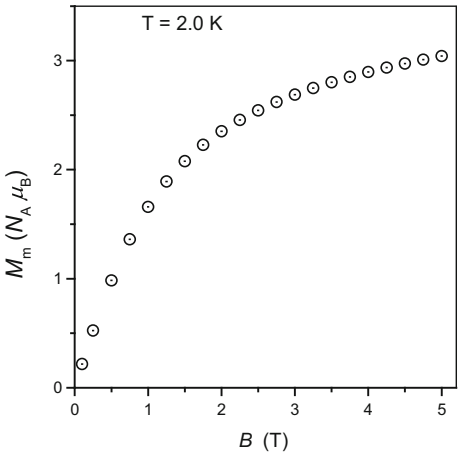

Fig. 3 Magnetometry data taken for sample **A**. Dependence of magnetization per Fe atom on magnetic field at 2 K

mean between the value at 5.0 T and the linear extrapolation to 10 T was considered as the saturation value. The value obtained that way, which has an estimated error margin of ±0.1–0.2 $N_A\mu_B$ due to the extrapolation, is 3.3 N_A μ_B for sample **A**.

We also estimated the magnetic moment per iron atom in sample **A** by using the relative contributions of the paramagnetic species as obtained from the analysis of the Mössbauer spectra (see Table 1). Using the spin-only magnetic moment, given by: $|\vec{\mu_S}| = g\mu_B\sqrt{S(S+1)}$ with S being the spin of the iron species present and keeping g=2 one obtains the magnetic moment of the corresponding species in terms of the Bohr magneton μ_B. For this calculation it was assumed that antiferromagnetic oxidic particles (represented by K1) as well as the diamagnetic species (contribution of K2 at 5 T, see Fig. 1b) do not contribute to the magnetic moment. K3 as a ferrous high spin species as well as K4 and K5 as ferric high spin species contribute to the total magnetic moment of the sample scaled to their relative contributions in the sample. The results are represented in terms of Bohr magneton. Using these assumptions for sample **A** a value of 3.1 $N_A\mu_B$ was obtained which corresponds quite well with the value 3.3 $N_A\mu_B$ obtained from magnetometry. In order to check for systematic errors sample **B** prepared by a liquid-phase technique was studied both by Mössbauer spectroscopy and magnetometry as well. Preparation conditions and analysis of sample **B** can be found in the Supporting Information. For this sample magnetometry yields 3.2 $N_A\mu_B$ and Mössbauer spectroscopy 3.3 $N_A\mu_B$ The results of both techniques are in good agreement, which supports the reliability of the present approach for the analysis of Mössbauer spectra of Fe species in zeolites.

The Mössbauer spectra of the used catalyst $\mathbf{A_{SCR}}$ are shown in Fig. 4. The most obvious observation is a strong increase in the Fe^{II} species after SCR. From the corresponding EPR spectrum displayed in Fig. 5 it is also evident that the contribution of the axial ferric high spin species located in the β-positions (g∼6) has been diminished drastically: it has almost disappeared. Therefore the almost axial S=5/2 species K5 was not included in the analysis of the Mössbauer spectra of $\mathbf{A_{SCR}}$. The analysis indeed reflects the partial reduction of the isolated Fe sites while the contribution of Fe^{II} increases from 3% to 35% of the total signal area (see Table 1).

In conclusion, we have measured Mössbauer spectra of Fe-ZSM-5 zeolites in low and high magnetic fields and consistently analyzed these data using relevant information

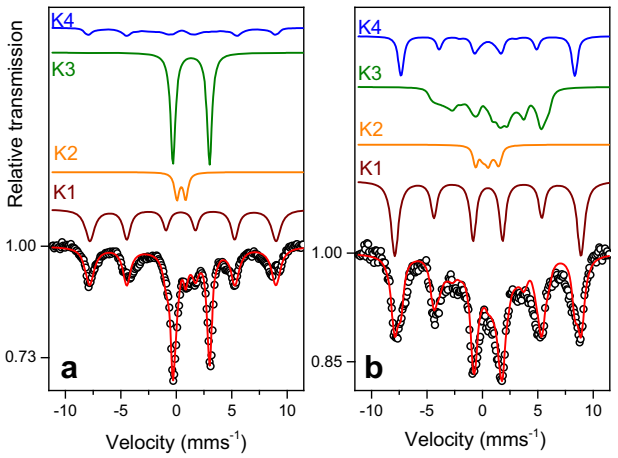

Fig. 4 Mössbauer spectra of sample A_{SCR} obtained at T=5 K and B=10 mT (**a**) and B=5 T (**b**). The red solid line is the result of a simulation procedure using 4 different iron species K1 – K4 as described in the text. The relative contribution of K1 – K4 including the obtained Mössbauer parameter sets are given in Table 1

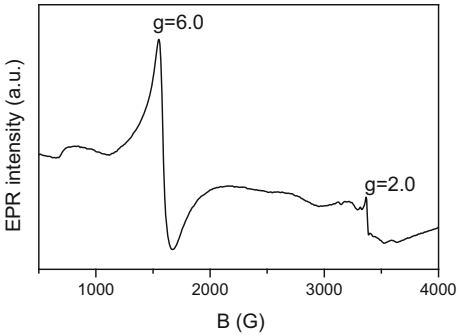

Fig. 5 X-band EPR spectrum of sample $\mathbf{A_{SCR}}$ taken at 90 K at a microwave frequency of 9.6 GHz

obtained from EPR spectroscopy. The combination with complimentary spectroscopic techniques like EPR spectroscopy allows quantifying the amount of paramagnetic iron sites in Fe-ZSM-5 and the detection of EPR-silent diamagnetic iron species like μ-oxo-bridged dinuclear iron sites even in these highly complex systems.

Acknowledgments V.S., A.B. and W.G. thank the DFG for funding under Schu 1251/15-2, BR 1380/18-2, GR 1447/21-2. The support of the research initiative NANOKAT is also acknowledged (V.S.).

References

1. Nova, I., Tronconi, E. (eds.): Urea-SCR Technology for deNOx Aftertreatment of Diesel Exhausts. Springer, Berlin (2014)
2. Grünert, W.: Active sites of selective catalytic reduction. In: Nova, I., Tronconi, E. (Eds.) Urea-SCR Technology for deNOx After Treatment of Diesel Exhausts, pp. 181–220. Springer, Berlin (2014)
3. Schwidder, M., Heikens, S., De Toni, A., Geisler, S., Berndt, M., Brückner, A., Grünert, W.: The role of NO2 in the selective catalytic reduction of nitrogen oxides over Fe-ZSM-5 catalysts: Active sites for the conversion of NO and of NO/NO2 mixtures. J. Catal. **259**, 96–103 (2008)

4. Devadas, M., Kröcher, O., Elsener, M., Wokaun, A., Mitrikas, G., Söger, N., Pfeifer, M., Demel, Y., Mussmann, L.: Characterization and catalytic investigation of Fe-ZSM5 for urea-SCR. Catal. Today. **119**, 137–144 (2007)
5. Koebel, M., Madia, G., Elsener, M.: Selective catalytic reduction of NO and NO2 at low temperatures. Catal. Today. **73**, 239–247 (2002)
6. Kumar, M.S., Schwidder, M., Grünert, W., Brückner, A.: On the nature of different iron sites and their catalytic role in Fe-ZSM-5 DeNOx catalysts: New insights by a combined EPR and UV/VIS spectroscopic approach. J. Catal. **227**, 384–397 (2004)
7. Berrier, E., Ovsitser, O., Kondratenko, E.V., Schwidder, M., Grünert, W., Brückner, A.: Temperature-dependent N2O decomposition over Fe-ZSM-5: Identification of sites with different activity. J. Catal. **249**, 67–78 (2007)
8. Čapek, L., Kreibich, V., Dědeček, J., Grygar, T., Wichterlová, B., Sobalík, Z., Martens, J.a., Brosius, R., Tokarová, V.: Analysis of Fe species in zeolites by UV-VIS-NIR, IR spectra and voltammetry. Effect of preparation, Fe loading and zeolite type. Microporous Mesoporous Mater. **80**, 279–289 (2005)
9. Pérez Vélez, R., Ellmers, I., Huang, H., Bentrup, U., Schünemann, V., Grünert, W., Brückner, A.: Identifying active sites for fast NH3-SCR of NO/NO2 mixtures over Fe-ZSM-5 by operando EPR and UV-vis spectroscopy. J. Catal. **316**, 103–111 (2014)
10. Dědeček, J., Kaucký, D., Wichterlová, B.: Co2+ ion siting in pentasil-containing zeolites, part 3. Co2+ ion sites and their occupation in ZSM-5: A VIS diffuse reflectance spectroscopy study. Microporous Mesoporous Mater. **35–36**, 483–494 (2000)
11. Schwidder, M., Kumar, M.S., Klementiev, K., Martina, M., Brückner, A., Grünert, W.: Selective reduction of NO with Fe-ZSM-5 catalysts of low Fe content I. Relat. Between Act. Site Struct. Catalytic Perform. **231**, 314–330 (2005)
12. Ellmers, I., Pérez Vélez, R., Bentrup, U., Schwieger, W., Brückner, A., Grünert, W.: SCR and NO oxidation over Fe-ZSM-5 – the influence of the Fe content. Catal. Today **258**, 337–346 (2015)
13. Schünemann, V., Paulsen, H.: Mössbauer spectroscopy. In: Scott, R.A., Lukehart, C.M. (eds.) Applications of Physical Methods to Inorganic and Bioinorganic Chemistry, pp. 243–270. Wiley (2007)
14. Ellmers, I., Vélez, R.P., Bentrup, U., Brückner, A., Grünert, W.: Oxidation and selective reduction of NO over Fe-ZSM-5 - How related are these reactions. J. Catal. **311**, 199–211 (2014)
15. Janoschka, A., Svenconis, G., Schünemann, V.: closed cycle-cryostat for high-field Mössbauer spectroscopy. J. Phys. Conf. Ser. **217**(1), 2010 (2005)
16. Gunnlaugsson, H.P.: Spreadsheet based analysis of Mössbauer spectra. Hyperfine Interac. **237**, 79 (2016)
17. Schünemann, V., Winkler, H.: Structure and dynamics of biomolecules studied by Mössbauer spectroscopy. Rep. Prog. Phys. **63**, 263–353 (2000)
18. Chen, H.-Y., Sachtler, W.M.H.: Catal. Today **42**, 73–83 (1998)